Hindawi
Mobile Information Systems
Volume 2022, Article ID 5446946, 10 pages
https://doi.org/10.1155/2022/5446946

Research Article

Visualization of the Residual Network for 3D Image Recognition considering the SVM Combined with the K-Nearest Neighbor Algorithm

Huabai Liu

Hunan Automotive Engineering Vocational College, Zhuzhou 412001, Hunan, China

Correspondence should be addressed to Huabai Liu; 164903302@stu.cuz.edu.cn

Received 5 May 2022; Accepted 20 July 2022; Published 11 August 2022

Academic Editor: Muhammad Muzammal

The support vector machine (SVM) combined with the *K*-nearest neighbor (KNN) algorithm is applied to the 3D image recognition algorithm to cope with the issues of 3D image recognition in the image processing process. In this paper, the KNN algorithm is used to extend the eigenvalues of the residual network from frequency to complex plane according to the eigenvalues of 3D images, and the relevant data are extracted from the images by using the corresponding separation rules of the SVM. Subsequently, a sparse observation model is established based on the SVM combined with the KNN, and the 3D image processing issue is converted to a residual network visualization issue of 3D image recognition by establishing a parameterized database. Meanwhile, detection of high-resolution distance of 3D images is conducted, and the variational inference method is used to visualize and analyze the 3D images accordingly. Finally, through the experimental study, it can be known that the method of SVM combined with the KNN algorithm can reach an accuracy of up to 94.18% in the dataset of the Princeton 3D polygonal models. After comparison with the existing SVM-KNN method and deep learning, it can be concluded that the method put forward in this paper has a higher recognition rate and stronger anti-interference capacity, and the algorithm has a superior convergence speed with less adjustment parameters.

1. Introduction

3D image recognition is one of essential methods used in the image processing industry at present, and it has been extensively applied in various industries and military fields. A 3D image is a carrier of information data transmitted, which contains the characteristics of the data source. 3D images are identified accurately and analyzed in detail. Data characteristics acquired from image processing can provide a basis to identify the sources of 3D image effectively. Currently, it is generally required that the characteristics of 3D image data selected should meet the conditions for time shift, size, and unchanged phase to ensure that they can be identified accurately [1, 2]. The visualization analysis of the image recognition residual network is extensively applied in different industry fields based on compliance with the above conditions. Meanwhile, it is also required to maintain a high level of noise resistance due to the relatively simple process of bispectral analysis and relatively low workload of operations, while keeping the spectral analysis at a relatively high order. It is more extensively used in the field of 3D image processing to obtain the bispectral quadratic characteristics in the complex diagonal direction of the images based on the visualization of quadratic characteristics of the residual network in the deep root 3D image recognition. Given that various high-performance computation subpaths are different in the accuracy of recognition, the application of SVM combined with the KNN algorithm can be implemented based on the characteristic vector of 3D images according to high-performance calculation. From the final experimental results, it can be seen that the proposed method can be applied to the secondary recognition algorithm for 3D image characteristics based on the criteria of baroclinic distance [3–5]. 3D images have been massively used in *s* high-resolution processing, characteristic extraction, image classification, and many other fields attributing to their superior all-day, real-time, long-range, and high-resolution features. In addition, the use of SVM combined with the KNN algorithm can improve the acquired high distance resolution, while reducing the transient bandwidth of the receiver, accomplishing the hardware reduction, and effectively shortening the observation time based on the subpulse carrier frequency sequence, thereby effectively improving the anti-interference performance of 3D images. 3D images mainly present the images of different factors (noise and images that play no significant role) fused together, and the transmission path is more complex. Even if a higher-functioning 3D image is used, it still fails to acquire ideal imaging results. It can be seen that the effective capture of original images with physical characteristics is challenging. Original images can be acquired by deconvolution based on the feedback from the fused image. This approach has been extensively used in different fields such as image processing, 3D images, speech, and medicine [6, 7]. Chan et al. put forward a more technologically advanced method, that is, the variational difference recovery method. According to this calculation method, the partial differential gradient projection is used to perform the Lagrange multiplier term and minimize the difference. As it is fast in convergence and stable, it is perfect for processing images with steep edges. The difference can be calculated according to the regular dynamic adaptive method.

In this paper, the 3D image recognition residual network is visualized and analyzed by the SVM combined with the KNN algorithm by converting the visualization parameter analysis of 3D image recognition into the evaluation issue of recognition analysis at the reconstruction joint.

The low signal-to-noise ratio (SNR) HRRP based on motion parameters of 3D image recognition in the search interval is used to implement the visualization parameter impact visualization analysis quickly and provided that HRRP reconstruction errors can be solved at a low SNR. The update speed of population is used to identify the local optimum to process 3D image visualization parameters accurately at last.

2. SVM Combined with the KNN Algorithm

According to the SVM combined with the KNN algorithm, it is mainly aimed at the problems that occur during the visualization of the residual network. If this problem is completely solved, it is necessary to use the SVM combined with the KNN algorithm to optimize the parameters of the 3D image recognition model [8, 9]. This paper also combines the strategy of K-means. K-means means that the SVM combined with the KNN algorithm is different from the conventional vector 3D image recognition model in terms of the connection method and parameter sharing method. The SVM combined with the KNN algorithm can implement local connection and data residual network sharing. Weight sharing mainly refers to the collection of parameter data according to multiple nodes in the hierarchical process. The feasibility analysis of shared data parameters is mainly related to multiple goals in the calculation process.

Different from the traditional method, the SVM combined with the KNN algorithm mainly uses the initial eigenvalues of the input signal of the collected data to visualize the input signal according to the hierarchy. Usually, the average time amplitude difference of the time-domain characteristics, the energy in a relatively short time, etc., are used as the initial input characteristics of the 3D image recognition model in this paper, and then $x(n)$ can be used for the 3D image recognition residual network signal. The short-term energy balance can be expressed as

$$\begin{aligned} E_n &= \sum_{m=-\infty}^{\infty} [x(n)w(n-m)]^2 \\ &= \sum_{m=-\infty}^{\infty} \left[x(m)^2 h(n-m)\right] \\ &= x(m)^2 * h(n). \end{aligned} \tag{1}$$

However, the high dimensionality of the time-domain characteristics under initialization will cause a lot of interference and noise. Therefore, the input visualization signal needs to be reduced in dimension.

At this time, the SVM combined with the KNN algorithm is used to conduct statistics on the multivariate of the survey, and the internal structure of the multivariate can be analyzed by studying multiple principal components. After the 3D image data are processed by dimensionality reduction, the input data residual network can be visualized, and the SVM-KNN algorithm in deep learning can process the output data. Among them, the visualization structure of the 3D image recognition residual network at this stage is shown in Figure 1.

In the 3D image residual network, the eigenvectors appear in different positions on the network visualization, and the importance of the performance of the network visualization ability is also different. This characteristic is described by the eigenvector level [10, 11]. If the characteristic vector TE appears n times in 3D image recognition, as in equation (2), in the characteristic vector grade score, T_K is the level of the eigenvector T appearing kth in 3D image recognition.

$$score(T) = \sum_{k=1}^{n} \frac{1}{2^{InT_k}}. \tag{2}$$

The eigenvector weights are

$$w(T) = score(T) \times idf_k. \tag{3}$$

In the case of calculating the weight similarity between the query Q and a certain news eigenvector word group D, due to the large amount of calculation and time overhead of the conventional SVM similarity, the ratio between weight value of the QD intersection part and the sum of the QD weight value are calculated.

$$sim(Q, D) = \frac{\sum_{k=1}^{|Q\cap D|}\left(w\left(T_{qk}\right) + w\left(T_{dk}\right)\right)}{\sum_{k=1}^{|Q|}\left(w\left(T_{qk}\right) + \sum_{k=1}^{|Q|} w\left(T_{dk}\right)\right)}. \tag{4}$$

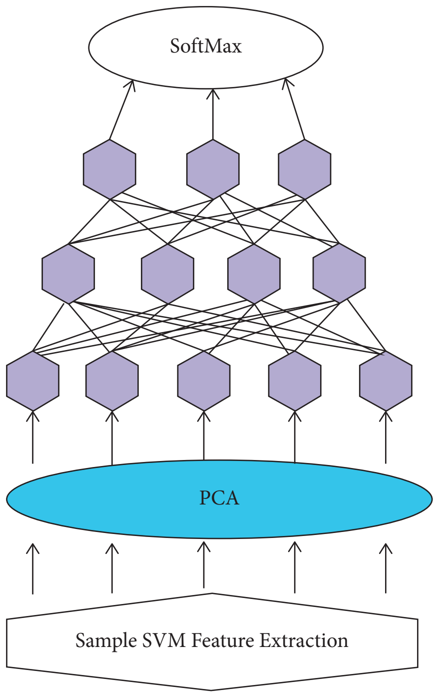

FIGURE 1: Residual network visualization vector space structure diagram.

The visualized 3D image residual network is extracted by using the support vector machine function. In case of any change in the mean value of the image pixel gray scale, the change will react to the support vector machine value of that column (row). The support vector machine function is expressed as follows:

$$M_v(x) = \frac{1}{y_2 - y_1}\int_{y_1}^{y_2} I(x, y)\mathrm{d}y,$$
$$M_h(y) = \frac{1}{x_2 - x_1}\int_{x_1}^{x_2} I(x, y)\mathrm{d}x. \tag{5}$$

In the expression, $I(x, y)$ is used to represent the pixel gray value of the residual network for 3D image recognition that can be obtained by calculation at the point (x, y); $M_v(x)$ stands for the vertical support vector machine corresponding to the interval $[y_1, y_2]$ in which it is set; and $M_h(y)$ stands for the horizontal support vector machine function used on the set interval. For the purpose of removing the external noise and interference in the image effectively, $M_v(x)$ and $M_h(y)$ are normalized to the interval of [0, 1] as

$$M_v'(y) = \frac{M_v(x) - \min(M_v(x))}{\max(M_v(x)) - \min(M_v(x))},$$
$$M_h'(x) = \frac{M_h(x) - \min(M_h(x))}{\max(M_h(x)) - \min(M_h(x))}. \tag{6}$$

In the task of performing determination on images through classification tools, a classification method by using a powerful support vector machine K-nearest neighbor algorithm to train small images is applied to carry out image discrimination. With regard to this type of image recognition skill, it is usually not general, where n samples are imported for image operation to form an $m \times n$ dimensional matrix; m stands for the number of data points in the image.

$$S_w = \sum_{i=1}^{k}\sum_{j\in N_i}\left(a_j - c^{(i)}\right)\left(a_j - c^{(i)}\right)^T,$$
$$S_b = \sum_{i=1}^{k}\sum_{j\in N_i}\left(c^{(i)} - c\right)\left(c^{(i)} - c\right)^T, S_t = S_w + S_b. \tag{7}$$

In the above equation, S_w stands for the residual network matrix of images; S_b stands for the interclass matrix of images; S_t stands for the full matrix; N_i stands for the number of images attributed to class i; n stands for the number of stock images; c stands for the mean value of the corresponding image; $c^{(i)}$ stands for the mean value corresponding to the ith class of images; and a_j stands for the j-th image.

The probability of the user multimedia residual network can be calculated. The purpose is to transform the residual network visualization vector space problem of a probabilistic 3D image recognition model as a problem of seeking conditional probability, presenting the diversification of user methods. The system automatically completes this coherent operation, and the user experience is not disturbed. First, the user history visualization residual network in the browser is saved, and the user's method is known, and then the user's method of visualizing the residual network is changed through the user's operation of the visualization result, and time labels are added to the data of the sense method. Therefore, by updating the user-insensitive method point [12] through the calculation equation of the SVM combined with the KNN algorithm and the number of occurrences and frequency of the support vector k_i in the 3D image recognition, its weight w_i is obtained:

$$w_i = tf_i \times idf_i, \tag{8}$$

where tf_i is the frequency of the support vector k_i in all visualized 3D images, and idf_i is the frequency of k_i in all visualized 3D images in the reverse order of 3D images. The calculation method is given in the following form:

$$idf_i = \log\frac{N}{n}. \tag{9}$$

It can be understood from the above analysis that the expression for the distance between the residual network and the class can be calculated by using the 3D image recognition residual network in the following form:

$$\mathrm{trace}(S_w) = \sum_{i=1}^{k}\sum_{j\in N_i}\left\|a_j - c^{(i)}\right\|_2^2,$$
$$\mathrm{trace}(S_b) = \sum_{i=1}^{k}\sum_{j\in N_i}\left\|c^{(i)} - c\right\|_2^2. \tag{10}$$

The initial image is reduced in dimensionality after being processed by the matrix $G^T \in R^{l\times m}$, which can be expressed in the high-dimensional space. Thus, the residual network, interclass, and overall scatter matrices can be expressed as follows:

$$\begin{aligned} S_w^Y &= G^T S_w G, \\ S_b^Y &= G^T S_b G, \\ S_t^Y &= G^T S_t G. \end{aligned} \tag{11}$$

Based on the criteria of the support vector machine K-nearest neighbor algorithm, the maximization of the interclass distances for $\mathrm{trace}(S_b^Y)$ can be achieved. As a result, the following variational optimization model can be obtained:

$$J(G) = \mathrm{trace}\left(\left(G^T S_w G\right)^{-1}\left(G^T S_w G\right)\right). \tag{12}$$

It is assumed that S_w is nonsingular, and then the following equation can be obtained:

$$\mathrm{trace}\left(\left(S_w^Y\right)^{-1} S_b^Y\right) \le \mathrm{trace}\left(S_w^{-1} S_b\right). \tag{13}$$

Thus, the upper limit of $J(G)$ can be deduced in the following form:

$$\mathrm{trace}\left(\left(S_w^Y\right)^{-1} S_b^Y\right) = \mathrm{trace}\left(S_w^{-1} S_b\right). \tag{14}$$

The matrix is composed of l eigenvector, for the maximum eigenvalue $G \in R^{m\times l}$ $S_w^{-1} S_b x = \lambda x$ before the equation, and if it is assumed that $l = k - 1$, as the evaluation results will not be detrimental to the quality of the evaluated clusters, the maximum $k - 1$ nonzero eigenvalues can be obtained. The judgment range of $J(G)$ has reached the nonanomalous value S_w when it is not sampled. In general, if the number of dimensions in the image data is greater than the number of images, it is singular. Hence, the method of QR decomposition and problem decomposition based on the generalized singular value is used to deal with the issue.

In the above equation, d is the eigenvector of the page, $F\colon R_n \longrightarrow R$ is the ith support vector of the current page, and $F\colon R_n \longrightarrow R$ is the weight of the support vector $F\colon R_n \longrightarrow R$ in page d.

NIN can also use the global averaging pooling layers without connecting all the classification layers and to take all the pooling layers with characteristics as the output values so that all characteristics can be mapped and identified directly [12, 13]. Thus, the network parameters can be reduced substantially, and each characteristic map will have their respective output characteristics, as shown in Figure 2. The global average pooling layers are added in the third and fourth layers of the NIN network structure, respectively.

Various indexes present at the same level are compared, and the comparison results are quantified according to the corresponding importance with reference to the criteria. Thus, the corresponding weights of the visualization indexes in the 3D image recognition residual network can be obtained. The specific steps are described as follows.

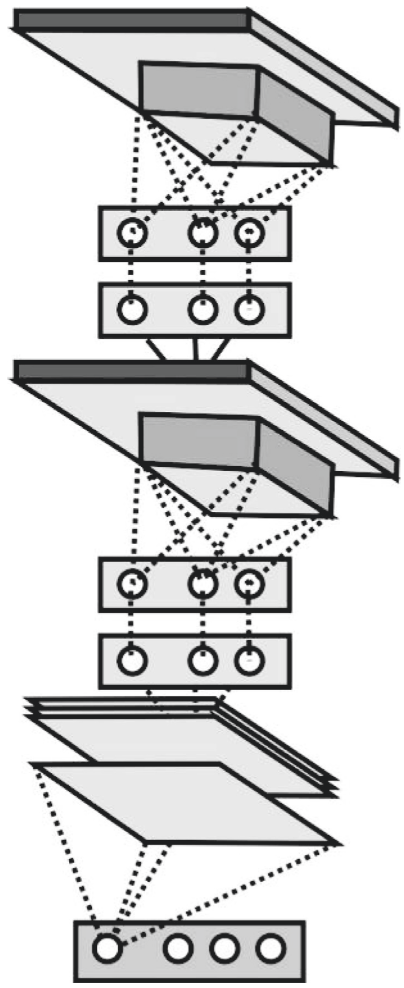

Figure 2: Overall framework structure of the NIN network.

After comparison with the indexes present in the same layer, the determination matrix A is established, which can be expressed as follows:

$$A = \begin{bmatrix} a_{11} & a_{12} & \cdots & a_{1n} \\ a_{21} & a_{22} & \cdots & a_{2n} \\ \vdots & \vdots & \vdots & \\ a_{n1} & a_{n2} & \cdots & a_{nn} \end{bmatrix}. \tag{15}$$

The judgment matrix is normalized by column, as shown in the following equation:

$$b_{ij} = \frac{a_{nn}}{\sum_{i=1}^{n} a_{nn}}. \tag{16}$$

The judgment matrix is normalized by row, as shown in the following form:

$$v_{ij} = \sum_{h=1}^{n} b_{ij}. \tag{17}$$

For the weights corresponding to the visual indexes of the talent development model, they can be calculated according to the equation in the following form:

$$w_i = b_{ij} \cdot \frac{v_i}{\sum_{i=1}^{n} v_i}. \tag{18}$$

The weight vector matrix W is established according to the weights of the visualization indexes in the 3D image recognition residual network obtained through calculation. Based on the visualization analysis data collected, the fuzzy matrix is constructed by calculating the degree of affiliation corresponding to the visualization present in the set of visualization analysis elements.

$$U_{mn} = \begin{bmatrix} U_{11}, U_{12}, U_{13}, U_{14}, U_{15} \\ U_{21}, U_{22}, U_{23}, U_{24}, U_{25} \\ \vdots \\ U_{m1}, U_{m2}, U_{m3}, U_{m4}, U_{m5} \end{bmatrix} W. \tag{19}$$

In the above equation, with regard to the annotated set, U_{ij}, U_j, and U_i stand for the degree of visualization and the degree of affiliation corresponding to the analysis factors.

The visualization model (F) for the 3D image recognition residual network can be obtained in accordance with the visualization degree obtained through calculation, and its expression is shown in the following form:

$$F = \frac{w_i \times U_{mn}}{U_j} \times \delta. \tag{20}$$

In the above equation, δ stands for the fuzzy operator.

2.1. SVM-KNN Network for 3D Image Recognition. The characteristic $r\ (i, j)$ that allows for the minimization of the SVM combined with the KNN algorithm is the desired characteristic [14]. Subsequently, the optimal image visualized as required is obtained through calculation of the coordinate difference between the two characteristics, r and $r\ (i, j)$. Based on the characteristic filtering criteria, each time the SVM combined with the KNN algorithm corresponding to the elements of the two characteristic arrays is calculated, and it is determined whether the result is larger than the minimum value at preset. If it is larger than the minimum value, the computation of the SVM combined with the KNN algorithm is suspended immediately. Thus, this characteristic is excluded accordingly. If it is less than the minimum value, the computation of the SVM combined with the KNN algorithm is continued.

The visualization method for the 3D image recognition residual network can be divided into visualization analysis element groups, and the expressions of the visualization analysis element groups are obtained as follows:

$$U = \{U_1, U_2, \cdots, U_m\}. \tag{21}$$

The primary evaluation analysis factor set for the visualization of the 3D image recognition residual network is further classified to obtain the secondary evaluation analysis factor set in the following form:

$$\begin{cases} U_1 = \{U_{11}, U_{12}, \cdots, U_{1n}\}, \\ U_2 = \{U_{21}, U_{22}, \cdots, U_{2n}\}, \\ \vdots \\ U_m = \{U_{m1}, U_{m2}, \cdots, U_{mn}\}. \end{cases} \tag{22}$$

Combined with the features of the visualization elements in the 3D image recognition residual network, the constraint model knowledge recognition algorithm is applied to the residual network visualization according to the actual situation in the visualization of the 3D image recognition residual network. In this way, the weights for the visualization of the layered residual network in each layer can be obtained effectively.

Equation(20) indicates that after n repetitions of the mode N from the initial value point (x_0, y_0), the result is expressed as the coordinate (x_n, y_n) after the conversion.

The visualization analysis is conducted on the 3D image recognition residual network. The diversity and accuracy are defined, and comprehensive evaluation is conducted to complete the visualization selectivity analysis of the 3D image recognition residual network [15–17]. Through the analysis of residual network visualization in 3D image recognition by composing 3D image recognition residual network visualization based on the particle swarm in the search space, the characteristic vector of the data information on the corresponding 3D image recognition residual network visualization can be expressed in the following form:

$$l_\varepsilon(g) = (1 - \rho) l_\varepsilon(g - 1) + \gamma f(\chi_i(g)), \tag{23}$$

where f is the adaptive function corresponding to the characteristic data characteristic vector χ_i of the 3D image recognition residual network visualization. $\gamma\chi_i(g)$ is the corresponding 3D image recognition residual network visualization analysis of the ε-th visualization in the practical application process.

The expression for the visualization π_p in the 3D image recognition residual network II is shown as follows[18]:

$$\mathrm{Acu}(\pi_p) = \mathrm{NMI}(\pi_p, \pi^*), \tag{24}$$

where π_p and π_q are the visualization of the 3D image recognition residual network. If there is less information shared with the visualization base cluster of the 3D image recognition residual network, the accuracy of this base cluster is relatively low. Otherwise, the accuracy of this base cluster is relatively high.

Based on the accuracy and diversity characteristics of the clusters for the visualization of the 3D image recognition residual network, the comprehensive evaluation criteria for defining clusters through the visualization of the 3D image recognition residual network can be defined in the following form:

$$\mathrm{Eval}(\pi_p) = \lambda \mathrm{Acu}(\pi_p) + (1 - \lambda) \mathrm{Div}(\pi_p), \tag{25}$$

where $\lambda \in [0, 1]$, and the visualization correctness and diversity of the 3D image recognition residual network are at a significant level according to the comprehensive evaluation criteria.

Equation(25) indicates that based on the diversity of the 3D image recognition residual network base visualization $\mathrm{Div}(\pi_p)$, the probability of selecting each 3D image recognition residual network base visualization algorithm is calculated and selected as the probability $\mathrm{pro}(\pi_p)$ of the optimized base visualization as follows:

$$\mathrm{pro}\left(\pi_p\right) = \frac{\mathrm{Div}\left(\pi_p\right)}{\sum_{p=1}^{B} \mathrm{Div}\left(\pi_p\right)}. \tag{26}$$

The computational results are used to select the visualization of the 3D image recognition residual network randomly based on roulette and to carry out analysis of the 3D image recognition residual network visualization.

In the SVM-KNN, the respective strengths of multilayer sensor residual networks and the SVM networks are leveraged. Among them, the SVM-KNN network has the following significant characteristics: (1) the volume kernel parameters and the sensor-related parameters can be used jointly in the sensor residual module with the same size. (2) Half of the volume kernel and sensor parameters that are present in this network are randomly generated by Gaussian distribution, and the remaining half are processed by using the construction of sparse matrices. Meanwhile, the Gaussian white noise is processed. (3) The network outputs the residual module of the sensor for pooling, mask layer characteristic acquisition, and multichannel integration of the classification parameters.

Figure 3 is the block diagram of SVM-KNN network structure designed in this paper. In the network, each visual projection pattern based on the 3D model can be fed into the same multilayer sensor residual network. It can be observed in Figure 3 that random MRU is generated randomly from the sensor residual module, and all the volume kernel parameters and sensor parameters in the constructed module are generated randomly and then normalized accordingly. The sparse MRU is mainly used as a sparse sensor residual module, and the volume kernel and sensor parameters in this module are mainly optimized with a sparse matrix based on a Gaussian white noise approach. In the network structure of the 3-channel MRU, when other channels are adjusted, only the number of volume kernels and the number of sensors is added to the new channel, and the rest of the structure remains unchanged.

The link weights and node biases of each layer are obtained by visual learning, and the network initialization is completed. Internet visualization requires a large amount of sample data and generates more parameter values. On the other hand, the problem of recommendation visualization based on 3D images lacks a large amount of sample data, and it takes a long time to visualize a large number of parameters, which is unfavorable for practical applications. During the calculation process, the eigenvector is used for the web page, and if the support vector weight We is determined by the TF $*$ IDF method and the word item is determined to be a named entity, the weight value shall be appropriately enhanced. The specific definition is given in the following form:

$$W_e = \begin{cases} \mathrm{idf}_e \times \alpha, & e \text{ is a named entity}, \\ \mathrm{idf}_e, & e \text{ is other}, \end{cases} \tag{27}$$

where α is the weighting factor, which is 5 in this experiment. If m words with large weights are selected to visualize the eigenvector of the web page, and the number of co-occurrence terms in the two-web page-characteristic vectors is used as the basis for judging similarity, and if the number of co-occurrences is greater than the threshold, then the two web pages are similar.

During the visualization of 3D image recognition residual network, according to the reasonable allocation of 3D image recognition residual network visualization resources in the system, the visualization quality of 3D image recognition residual network can be effectively improved. The energy consumed by the data transmission node in the 3D image recognition residual network in transmitting k-bit data to node d can be expressed as follows:

$$E_{TX}(k,d) = \begin{cases} E_{\mathrm{TX-elec}} \cdot k + \varepsilon_{fs} \cdot d^n \cdot k, \\ E_{\mathrm{TX-elec}} \cdot k + \varepsilon_{mf} \cdot d^n \cdot k. \end{cases} \tag{28}$$

After the transmission energy loss is calculated, the width of the data transmission network can be calculated and allocated reasonably according to the actual resource data. The equation for the width of the network gradient is as follows:

$$B_r = \frac{L}{M}\left(1 + \alpha \frac{2m - M}{2M}\right), \tag{29}$$

where L is the maximum transmission distance between nodes; M is the maximum network gradient; m is the network gradient; α and β adjust the transmission radius of the competing cluster according to the calculation result of the network gradient width, and the transmission radius of node i is as follows:

$$A(i) = \beta \cdot r_i \cdot B_r \cdot \frac{m}{M}, \tag{30}$$

where β is the transmission radius adjustment coefficient and r_i is the initial transmission radius of the node. Therefore, the transmission energy gain of node i is given as

$$\mathrm{GaE}(i) = A(i)\left[E_{\mathrm{ar}}(i) - E_{co}(i)\right], \tag{31}$$

where $E_{cr}(i)$ and $E_{co}(i)$, respectively, are the energy received and the energy consumed by the node. Then the final 3D image recognition residual network visualization resource data allocation equation is

$$W(i) = \frac{1}{A(i)} - \frac{\mathrm{GaE}(i)}{\max(\mathrm{GaE}(i)) - \min(\mathrm{GaE}(i))}, \tag{32}$$

where $\max(\mathrm{GaE}(i))$ and $\min(\mathrm{GaE}(i))$, respectively, are the maximum and minimum values of the working energy of node i.

3. Experimental Analysis and Results

The SVM combined with the KNN algorithm designed in this paper mainly uses Microsoft Visual Studio 2008 as the tool for algorithm development, borrows SQL Server 2005

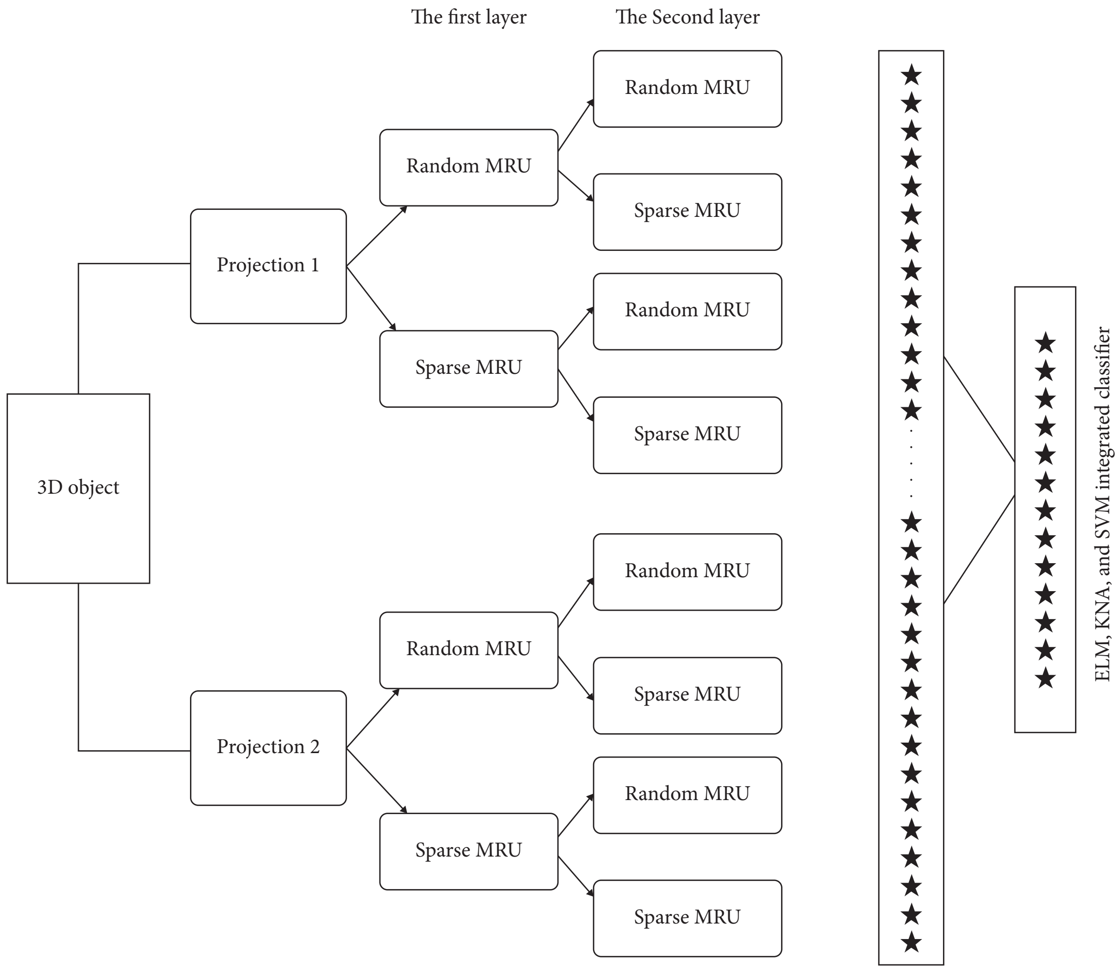

Figure 3: Network structure of the recognition of 3D images based on the SVM-KNN.

as the research database, and uses the three-layer B/S (Browser/Web Server/Database Server) framework for the algorithm framework [19]. The algorithm can provide effective network services for users and background managers. In the case of using the SVM combined with the KNN algorithm, the design of the SVM combined with the KNN algorithm can be completed. The learning resources that can be obtained by this algorithm mainly include online electronic courses, 3D image recognition residual network visualization of course videos, and electronic resources. Different kinds of resources can also be "encapsulated." The SVM combined with the KNN algorithm can not only provide Internet services for users but also provide other information network services. A specific language framework is used to complete the development of different modules, combined with the SVM with the KNN algorithm, to share network resources and to reduce resource waste and excessive developments much as possible [20, 21].

In general, there are many factors that affect the recognition accuracy of the algorithm, such as the different selection angles of the 3D image projection viewing angle, the number of channels of the sensor residual module, and the reliability threshold of the classification layer. In order to detect the recognition accuracy that can be achieved by different factors, this paper adopts the strategy of controlling variables in the experimental process to find all optimal network parameter values and obtain the optimal test results.

The visual energy consumption results in Figure 4 suggest that the total processing time spent by the SVM combined with the KNN algorithm is always kept at a low value while the residual network data continue to increase, the residual network data information continue to increase, and the energy spent by the algorithm in transmission remains low. It can be shown that the data energy consumption of residual network resources in the algorithm is less affected by the data scale. However, the visual energy consumption of the method used in reference [4] changes significantly with the continuous increase of the scale of data information, which shows that the energy consumption of the method used in reference [4] is unstable. The visualization time under the method in reference [5] can be kept stable. However, the total energy consumption of this algorithm is greater than the algorithm design value. Hence, the SVM combined with the KNN algorithm designed in this paper is superior in data processing capacity.

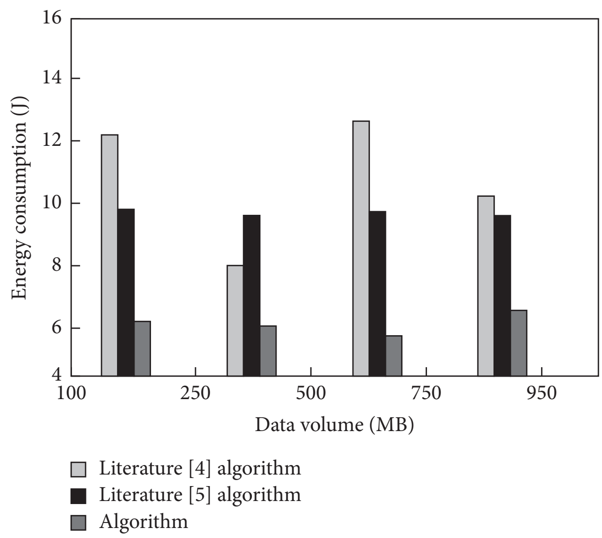

Figure 4: Visualized energy consumption comparison results.

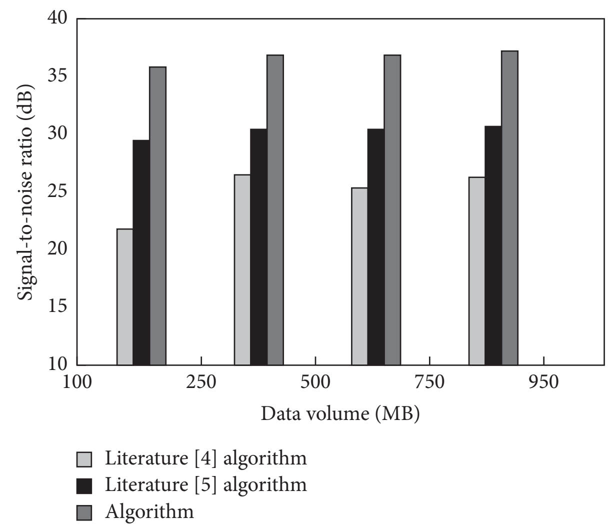

Figure 5: Results of transmission SNR comparison.

As shown in Figure 5, the analysis indicates that the design algorithm has good performance due to its higher transmission SNR of network resources than the other two algorithms in the literature. The visualization effect of residual network based on the traditional algorithm and the SVM combined with the KNN algorithm is compared and analyzed. Based on a usage score of 500 points, as shown in Table 1, the performances of the two visualization algorithms are compared.

Table 1: Comparative analysis of the two methods for remote 3D image recognition residual network visualization acquisition scores.

Number of users	Traditional algorithm	SVM combined with the KNN algorithm
200	300	450
400	280	480
600	285	485
800	270	475
1000	265	475

Table 1 indicates that if the number of users is 200, the maximum score is set to 300 using the previous algorithm. If the number of users is 1000, the minimum score is set to 265 using the previous algorithm. When the number of users is 600, the visualization of the 3D image recognition residual network using the SVM combined with the KNN algorithm reaches the highest score of 485 points. When the number of users is 200, the minimum score of 450 is obtained using the SVM combined with the KNN algorithm. In summary, by using the SVM-KNN algorithm for the visualization of the residual network of 3D image recognition, the learning interest can be more stimulated.

The comparison and analysis results of network visualization efficiency between two algorithms are shown in Figure 6.

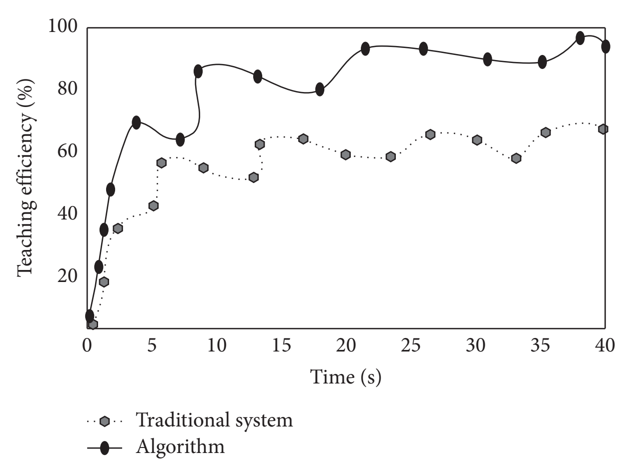

Figure 6: Comparative analysis of the visualization efficiency of the two algorithms for the 3D image recognition residual network.

Figure 6 indicates that if the time is 10 s, the network visualization efficiency using the traditional algorithm is 59.9%, and the network visualization efficiency using the SVM combined with the KNN algorithm is 88%. When the time is 20 s, the network visualization efficiency using the traditional algorithm is 61%, and the network visualization efficiency using the SVM combined with the KNN algorithm is 91%. When the time is 30 s, the network visualization efficiency using the traditional algorithm is 92%, and the network visualization efficiency using the SVM combined with the KNN algorithm is 61%. When the time is 40 s, the network visualization efficiency using the traditional algorithm is 93%, and the network visualization efficiency using the SVM combined with the KNN algorithm is 62%. Both initial algorithms were affected by the delay, and the network visualization efficiency decreased. After that, the KNN algorithm based on the SVM started faster and quickly returned to the normal mode. As mentioned above, the design of the 3D image recognition residual network visualization of the SVM-KNN algorithm is reasonable.

4. Conclusion

The bispectral analysis characteristics in the identification of individual data sources are extracted, and their quadratic features are optimized under SVM criteria through the in-depth analysis on residual network visualization for the identification of 3D images. This method can identify the bounded deviation and obtain the values of the observation error quickly, which has effectively implemented the complexity calculation of variation parameters. The experimental results have verified the effectiveness of the proposed method, which can restore data of original images in a background with low SNR. The images are processed according to the statistical characteristics of scattered points and noise. Through practical analysis, it can be seen from the experimental results that the usage time can be reduced by the method, which is suitable for processing multiple types of 3D images as well. The characteristics of data acquired at a low SNR always have excellent robustness. The visualization rate of 3D images based on recognition residual network is above 90% at an SNR of 0. However, the methods of individual recognition based on bispectral analysis generally have the common defect of a low recognition rate. The detailed features of images can be integrated to further improve the practical effectiveness of the algorithm through the characteristic vector. Compared with the other methods, the efficiency of the algorithm 3D image recognition residual network visualization put forward in this paper is quite fast. In the future, it is necessary to further investigate deeper and more perspectives of the perceptron residual SVM-KNN algorithm to obtain superior results.

Data Availability

The data used to support the findings of this study are available from the corresponding author upon request.

Conflicts of Interest

The authors declare no conflicts of interest.

Acknowledgments

This research study was sponsored by Hunan Province Education Science "Thirteenth Five-Year Plan" 2020 Annual Project (Subject category: general funded subject). The name of the project is Research on the Construction of Art Design Professional Groups in Hunan Higher Vocational Colleges Based on the 1+X Certificate System. The project number is XJK20BZY022. The authors are thankful to them for supporting this article!

References

[1] A. Sinha, A. Unmesh, Q. Huang, and K. Ramani, "Surfnet: generating 3d shape surfaces using deep residual networks," *IEEE Computer Society*, vol. 7, no. 4, pp. 1–14, 2017.

[2] Z. Shi, G. Zeng, L. Zhang, X. Zhuang, L. Li, and G. Yang, "Bayesian voxdrn: a probabilistic deep voxelwise dilated residual network for whole heart segmentation from 3d mr images," *Springer Cham*, vol. 7, no. 3, pp. 1–14, 2018.

[3] E. T. Nykaza, A. P. Boedihardjo, Z. Wang et al., "Deep learning for unsupervised feature extraction in audio signals: m," *Journal of the Acoustical Society of America*, vol. 140, no. 4, p. 3424, 2016.

[4] N. Brancati, G. De Pietro, D. Riccio, and M. Frucci, "Gigapixel histopathological image analysis using attention-based neural networks," *IEEE Access*, vol. 9, no. 9, pp. 87552–87562, 2021.

[5] Y. Zhao, P. W., J. Wu, H. Li, and K. Shi, "A 3d deep residual convolutional neural network for differential diagnosis of parkinsonian syndromes on 18 f-fdg pet images," *Annual International Conference of the IEEE Engineering in Medicine and Biology Society*, vol. 9, no. 6, pp. 1–14, 2019.

[6] C. Cao, K. Sun, and W. Liu, "A novel bit-level image encryption algorithm based on 2d-licm hyperchaotic map," *Signal Processing*, vol. 143, no. 3, pp. 122–133, 2018.

[7] Y. Chen, "Sports sequence images based on convolutional neural network," *Mathematical Problems in Engineering*, vol. 2021, no. 4, pp. 1–14, 2021.

[8] K. F. Wang, S. Zhuang, and X. R. Zhao, "JPEG image encryption algorithm based on three-dimensional multi-chaotic system," *Applied Mechanics and Materials*, vol. 734, pp. 554–557, 2015.

[9] M. Xu, C. Zou, R. Liang, W. Li, and Q. Wang, "Characteristic extraction and recognition of auditory attention in middle latency response from single electrode," *Journal of Southeast University*, vol. 47, no. 3, pp. 432–437, 2017.

[10] X. Chen, J. Li, Y. Zhang, Y. Lu, and S. Liu, "Automatic characteristic extraction in x-ray image based on deep learning approach for determination of bone age," *Future Generation Computer Systems*, vol. 26, no. 6, pp. 1–20, 2020.

[11] N. Stahl, G. Mathiason, G. Falkman, and A. Karlsson, "Using recurrent neural networks with attention for detecting problematic slab shapes in steel rolling," *Applied Mathematical Modelling*, vol. 70, no. 4, pp. 365–377, 2019.

[12] K. Qian, L. Tian, Y. Liu, X. Wen, and J. Bao, "Image robust recognition based on characteristic-entropy-oriented differential fusion capsule network," *Applied Intelligence*, vol. 20, no. 2, pp. 506–515, 2020.

[13] S. Halagowda and S. K. Lakshminarayana, "Image encryption method based on hybrid fractal-chaos algorithm," *International Journal of Intelligent Engineering and Systems*, vol. 10, no. 6, pp. 221–229, 2017.

[14] L. Sergey, M. Vasiliy, K. Innokentiy, and K. Victor, "A spiking neural network in semg characteristic extraction," *Sensors*, vol. 15, no. 11, pp. 27894–27904, 2015.

[15] X. Dai, J. Cheng, Y. Gao et al., "Deep belief network for feature extraction of urban artificial targets," *Mathematical Problems in Engineering*, vol. 2020, no. 10, pp. 1–13, 2020.

[16] H. Amakdouf, M. El Mallahi, A. Zouhri, A. Tahiri, and H. Qjidaa, "Classification and recognition of 3d image of charlier moments using a multilayer perceptron architecture," *Procedia Computer Science*, vol. 127, no. 6, pp. 226–235, 2018.

[17] M. Dong, Z. Fang, Y. Li, S. Bi, and J. Chen, "Ar3d: attention residual 3d network for human action recognition," *Sensors*, vol. 21, no. 5, p. 1656, 2021.

[18] B. Sun, "Attention feature network extraction combined with the generation algorithm of multimedia image description," *Advances in Multimedia*, vol. 2021, p. 8, 2021 6484128.

[19] S. Sun, W. Wang, Z. Peng, and J. Yang, "Rna inter-nucleotide 3d closeness prediction by deep residual neural networks," *Bioinformatics*, vol. 37, no. 8, pp. 1093–1098, 2020.

[20] M. Ran, J. Hu, Y. Chen et al., "Denoising of 3d magnetic resonance images using a residual encoder-decoder wasserstein generative adversarial network," *Medical Image Analysis*, vol. 55, no. 9, pp. 165–180, 2019.

[21] D. B. Miller, W. B. Glisson, M. Yampolskiy, and K. K. R. Choo, "Identifying 3d printer residual data via open-source documentation," *Computers & Security*, vol. 75, no. 7, pp. 10–23, 2018.